

Bamboo Fibers @ Poly(ethylene glycol)-Reinforced Poly(butylene succinate) Biocomposites

Le Bao, Yiwang Chen, Weihua Zhou, Yang Wu, Yulan Huang

Institute of Polymers, Nanchang University, 999 Xuefu Avenue, Nanchang 330031, China

Received 9 December 2010; accepted 15 February 2011

DOI 10.1002/app.34365

Published online 20 June 2011 in Wiley Online Library (wileyonlinelibrary.com).

ABSTRACT: The poly(poly(ethylene glycol) methyl ether methacrylate)- (PPEGMA)-grafted bamboo fiber (BF) (BF@PPEGMA) was successfully synthesized via the esterification and atom transfer radical polymerization (ATRP) methods. The poly(butylenes succinate) (PBS) matrix-based composites including BF and BF@PPEGMA were prepared by a twin-screw extruder. The structure, morphology, as well as the properties of BF@PPEGMA and composites was investigated. The results indicated that PPEGMA was successfully grafted onto the BF surfaces, making BF surfaces rough and less thermally stable. The BF@PPEGMA showed of stronger interactions with PBS matrix than pristine BF,

leading to the improvement of tensile modulus, tensile strength, and elongation at break of the composites. The PBS/BF@PPEGMA composites absorbed less water than PBS/BF composites due to the existence of less content of hydroxyl groups after surface modification. Incorporation of BF and BF@PPEGMA facilitated the crystallization of PBS at higher temperatures, leading to formation of regular spherulites without appearance of transcrystallization. © 2011 Wiley Periodicals, Inc. *J Appl Polym Sci* 122: 2456–2466, 2011

Key words: bamboo fibers; poly(butylenes succinate); composites; ATRP

INTRODUCTION

In recent years, the natural fiber-reinforced biocomposites have received more and more attention due to the economic and ecological pressure to conserve petroleum resources.¹ The natural fibers are renewable, cheap, and environmentally friendly, exhibiting low density with acceptable specific mechanical properties. In addition, the polymer matrix is also renewable, which makes the whole composite system ecofriendly.²

Among the natural plant fibers, bamboo fiber (BF) has attracted worldwide attention as a potential reinforcement of polymer composite because of its inborn properties such as low density, high tensile modulus, low elongation at break.^{3–5} Its specific stiffness and strength are comparable to those of glass fiber. Bamboo fiber composites with different polymers including epoxy resin,⁶ polypropylene (PP),⁷ polyvinyl chloride (PVC),⁸ poly(butylenes succinate) (PBS),⁹ and polylactic acid (PLA)¹⁰ have been reported by

many researchers. The results indicated that the incorporation of bamboo fibers could significantly improve the tensile strength and elastic modulus of the polymer matrix. The crystallization, thermal behavior, as well as the degradation of polymer was also affected by the existence of bamboo fibers.

However, similar to the other plant fibers, the bamboo fibers are hydrophilic due to the existence of large amount of hydroxyl groups on the surfaces of the fibers. It is therefore unreasonable to blend bamboo fibers directly with hydrophobic polymer because of the poor interfacial bonding between the fiber and the polymer matrix. As is known, the properties of composites are significantly controlled by the interface between the reinforced fibers and the matrix.¹¹ In most early works on the development of composite, the fiber-matrix interface was considered to be critical for ensuring good composite mechanical properties.^{12,13} Thus, the majority of the researchers were focused on the surface modification of bamboo fibers to improve the interfacial adhesion between the fibers and polymer matrix.¹⁴ Among the different methods of surface modification, the alkali treatment and acid treatment were frequently used to improve the compatibility between fiber and polymer matrix. The silane coupling agent was found to significantly improve the impact fatigue strength of the composites. As reported by Zhang et al.,¹⁵ they incorporated maleic anhydride polypropylene (MAH-PP) into the PP/PLA/BF composites to bring about beneficial changes in morphology and rheological properties.

Correspondence to: Y. Chen (ywchen@ncu.edu.cn) or W. Zhou (dramzwh@126.com) or Y. Wu (wuyang@ncu.edu.cn).

Contract grant sponsor: Natural Science Foundation of Jiangxi Province; contract grant numbers: 2009GQH0068, 2009GQC0086.

Contract grant sponsor: Program for Innovative Research Team in University of Jiangxi Province.

The dispersion of PLA in PP, as well as the bamboo fiber matrix interactions was also improved. Lee et al.¹⁰ used the lysine-based diisocyanate (LDI) as a coupling agent for the PLA/BF and poly(butylene succinate) (PBS)/BF composites. The tensile properties, water resistance, and interfacial adhesion of both PLA/BF and PBS/BF composites were improved by the addition of LDI. The other techniques focused on the grafting of different monomers via copolymerization onto the surfaces of the fibers, including free radical polymerization,¹⁶ ring-opening polymerization,¹⁷ nitroxide-mediated polymerization (NMP),¹⁸ RAFT,¹⁹ and ATRP.²⁰ Among the above techniques, ATRP allows the synthesis of polymer with predefined molecular weight and narrow molecular weight distribution. Therefore, it was extensively studied for graft copolymerization of vinyl monomers onto fibers in a living/controllable way.

As is known, the PBS is a biodegradable polymer based on butanediol and succinic acid which may be soon available from bio-based renewable resources. Furthermore, PBS shows the melting point similar to that of LDPE and tensile strength between PE and PP, as well as excellent processing capabilities. Combination of PBS and bamboo fibers is a reasonable way to produce composites based on the renewable resources. The PBS/BF composite has been reported by Kori⁹ and Lee,¹⁰ however, Kori mainly focused on the crystallization behavior and viscoelasticity of the composites. Lee investigated the effect of bio-based coupling agent LDI on the properties of PBS/BF composites but LDI is expensive and somehow unstable in moisture condition. How to improve the impregnation and interfacial bonding between PBS matrix and BF is a critical problem in manufacturing of composites. Since ATRP is able to incorporate of polymers with predetermined molecular weight onto the surfaces of particles, fibers or membranes, the bamboo fibers could also be modified by this method. The grafted polymer is believed to be compatible with PBS matrix and shows strong interaction between PBS matrix and BF. Furthermore, the moisture absorption of BF could also be limited by the incorporation of polymers. Poly(ethylene oxide) (PEO) is known to be completely miscible with PBS in all compositions, and the PEO remained in the lamellar region of crystalline PBS at PEO content lower than 20 wt %.²¹ Thus, the polymers containing PEO segments are supposed to be compatible and exhibit strong interaction with PBS. As far as we know, the incorporation of poly(poly(ethylene glycol) methyl ether methacrylate) (PPEGMA) onto the surfaces of BF via ATRP has not been reported. In this article, the BF@PPEGMA was prepared to improve interfacial adhesion between BF and PBS. The corresponding thermal and tensile properties, morphology, crystallization and melting behaviors,

as well as water absorption behavior of the PBS/BF@PPEGMA composites were analyzed.

EXPERIMENTAL

Materials

Poly(butylene succinate) with a number-average molecular weight (M_n) of 100,000 g/mol was supplied by Anqing Hexing Chemical Co., Ltd (China). Bamboo fibers were purchased from Liukexing Textile Co., Ltd (Shanghai, China). The fibers were cut to 3–5 mm length, and then dried at 70°C under vacuum for 48 h. Tetrahydrofuran (THF), triethylamine, acetone, and ethanol was purchased from Tianjin Damao Chemical Reagent Factory of China. 2-Bromoisobutryl bromide (BIBB), 4-dimethyl aminopyridine, 2,2'-bipyridyl (Bpy), poly(ethylene glycol) methacrylate (PEGMA) macromonomer ($M_n = 300$) were purchased from Aldrich. Copper(I) bromide (CuBr) was purified by stirring with glacial acetic acid, followed by washing with ethanol and acetone and drying at 40°C under vacuum for 24 h. THF was distilled over potassium before use. The other reagents were used directly without further purification.

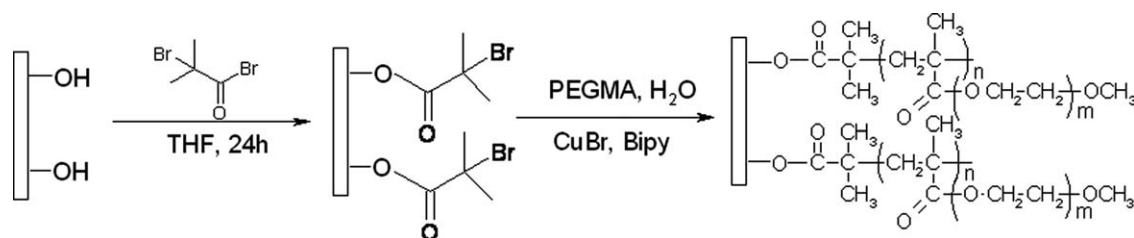
Preparation of BF@PPEGMA

The process for preparation of BF@PPEGMA was illustrated in Scheme 1. First, 1.5 mL of triethylamine and a catalytic amount of 4-dimethyl aminopyridine of 10 mg were charged into a 500 mL flask containing 220 mL of THF and 5 g bamboo fibers under nitrogen protection. The mixture was cooled to 0°C, followed by the addition of BIBB by dropwise under vigorous stirring. Then, the mixture was heated to room temperature and stirred for 24 h. The received BIBB-immobilized BF was washed by THF, ethanol and ultrasonicated for several times to remove the unbounded species. Consequently, the BIBB-immobilized BF was dried under vacuum at 70°C for 24 h.

The received BIBB-immobilized BF, PEGMA, and deionized water were charged into the pyrex tube under nitrogen protection. After stirring for 15 min, CuBr and Bpy were added. Then, the mixture was poured into ethanol after reacting at 30°C for 24 h, followed by washing with deionized water for five times and drying under vacuum at 70°C for 24 h. Finally, the BF@PPEGMA was obtained, and the weight ratio of grafted PPEGMA to BF was determined to be about 49.0%.

Fabrication of PBS/BF composites

To prepare the PBS/BF composites, PBS and BF were dried under vacuum at 60°C for 24 h before



Scheme 1 Synthesis procedure of PPEGMA-grafted bamboo fibers.

use. Then, PBS and BF with different ratios were mixed and extruded by a twin-screw extruder (SJSZ-10, Wuhan Ruiming Co., China) at 140°C and with a screw speed of 35 rpm. The received samples were then fabricated into standard specimens by an injection molding machine (SZ-15, Wuhan Ruiming Co., China) with a 4-mm-wide dog-bone-shape strips, with the grip-to-grip distance of 70 mm and thickness of 2 mm. The BF content in PBS was 1%, 5%, 10%, and 15% in weight, respectively.

Water absorption of PBS/BF composites

The samples were dried under vacuum at 70°C for 24 h, followed by cooling in a desiccator containing silica gel. After obtaining the weight of samples, they were immersed in deionized water for 192 h (25°C). At different time scale, the specimens were taken out, followed by removing of the excess water with tissue paper and weighing of the specimens. Water absorption was calculated by the following equation:

$$\text{Water absorption (\%)} = (W_f - W_i) / W_i \times 100\%$$

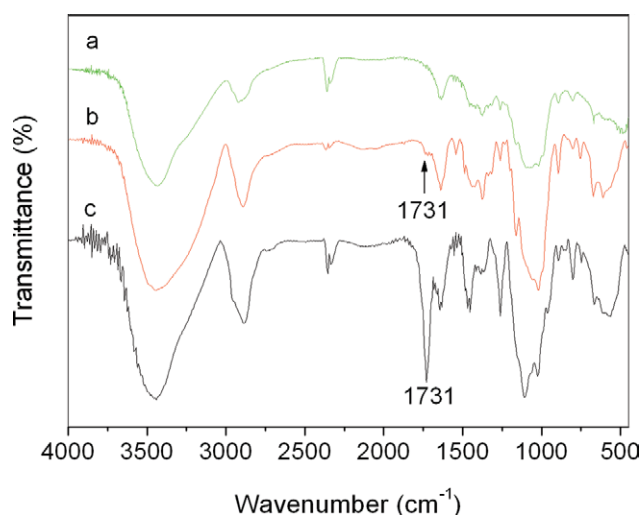


Figure 1 FTIR spectra of (a) pristine BF, (b) BIBB-immobilized BF, and (c) BF@PPEGMA. [Color figure can be viewed in the online issue, which is available at wileyonlinelibrary.com.]

where W_f and W_i are the weight of wet and dried samples, respectively.

Characterization

The Fourier transform infrared (FTIR) spectra were measured on a Shimadzu IRPrestige-21 FTIR spectrophotometer. X-ray photoelectron spectroscopy (XPS) was performed on Kratos AXIS Ultra, operating at 15 kV and 15 mA with an alumina target (Al Ka, $h\nu = 1486.71$ eV). The cross section morphology of membranes were investigated by scanning electron microscope (SEM), using an Environmental Scanning Electron Microscope (ESEM, FEI Quanta 200F). All samples were soaked in liquid nitrogen and fractured, followed by sputtering of a thin layer of gold. The cross section of the samples was then observed by SEM with an accelerating voltage of 20 kV. Thermal gravimetric analysis (TGA) was performed using a Perkin-Elmer instrument PYRIS DIAMOND at the heating rate of 10°C min⁻¹ under a nitrogen atmosphere (50 mL min⁻¹). Tensile strength, elongation at break, and elastic modulus were measured with a CMT8502 Machine model GD203A (Shenzhen Sans Testing Machine Co., Ltd, China) at a speed of 20 mm min⁻¹. The strain gauge was used during testing process and at least five samples were tested. The crystallization and melting behaviors of samples were performed on a Shimadzu DSC-60 calibrated with indium and zinc standards. The samples of about 5 mg were annealed at 150°C for 3 min to erase the thermal history. Then, samples were cooled to -50°C at a rate of 10°C/min and subsequently heated to 150°C at a rate of 10°C/min. The corresponding cooling and heating curves were then recorded. The crystallization temperature (T_c), melting temperature (T_m), crystallization enthalpy (ΔH_c), as well as the melting enthalpy (ΔH_m) were also recorded. For polarized optical micrograph (POM) observation, the specimens were heated to 150°C for 3 min and cooled rapidly to 80°C and crystallized for 1 h. Then, the specimens were rapidly cooled to room temperature to observe the morphology by polarized optical microscope (Nikon E600 POL) equipped with a camera.

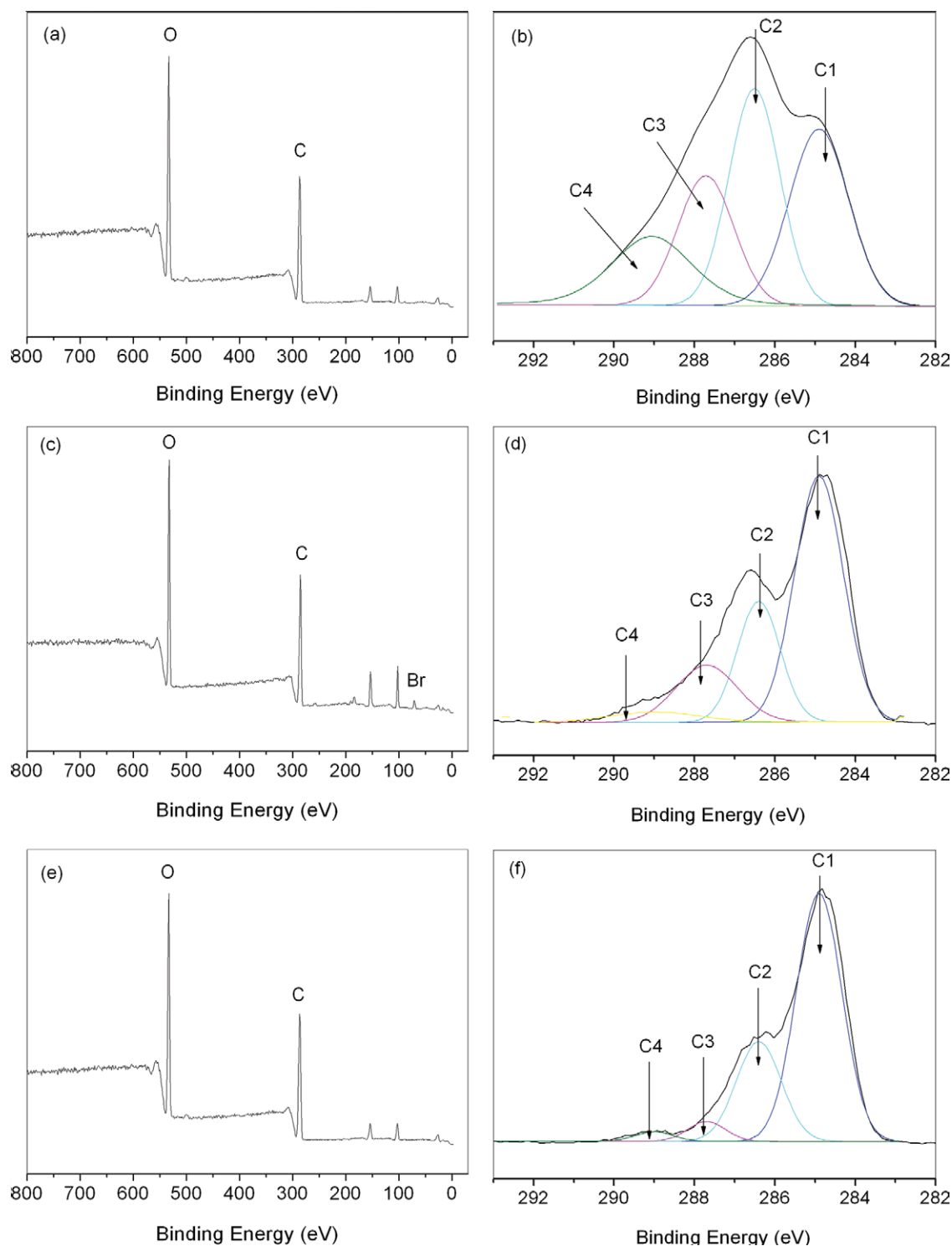


Figure 2 XPS wide scan and C1s core-level spectra of (a) and (b) the pristine BF, (c) and (d) BIBB-immobilized BF, and (e) and (f) BF@PPEGMA. [Color figure can be viewed in the online issue, which is available at wileyonlinelibrary.com.]

RESULTS AND DISCUSSION

Structure and morphology of BF@PPEGMA

Bamboo fibers are known to contain a large amount of hydroxyl groups on the surfaces. In this article, as shown in Scheme 1, some of the hydroxyl groups were first converted to 2-bromoisobutyryl groups

via esterification. The bromoisobutyryl groups were then served as the initiator to induce ATRP of PEGMA on BF. The structure of modified BF was analyzed by FTIR as shown in Figure 1. When compared with pristine BF, the BIBB-immobilized BF shows a new peak at about 1731 cm^{-1} , attributed to absorption of carbonyl groups. It is indicated that

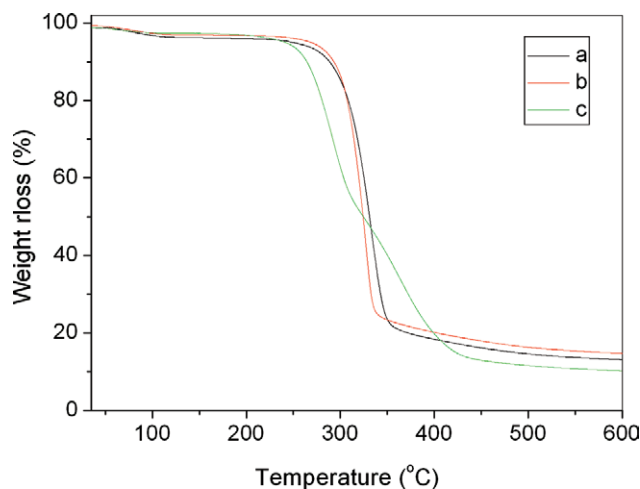


Figure 3 TGA curves of (a) pristine BF, (b) BIBB-immobilized BF, and (c) BF@PPEGMA. [Color figure can be viewed in the online issue, which is available at wileyonlinelibrary.com.]

the bromoisobutyryl groups were anchored onto the surface of BF via esterification. Furthermore, the absorption peak at 1731 cm^{-1} of BF@PPEGMA becomes stronger, showing that the PPEGMA has been successfully grafted onto BF via ATRP.

The chemical compositions of the surfaces of the bamboo fibers were further analyzed by XPS as shown in Figure 2. In the wide scan spectrum of the samples, it is noted that the pristine BF exhibits two characteristic peaks of carbon (285 eV) and oxygen (533 eV), which is consistent with the results reported previously [Fig. 2(a)].²² It is further noticed that the photoelectron line at binding energy (BE) about 70 eV, attributed to the Br 3 days was observed for the BIBB-immobilized BF [Fig. 2(c)]. It is suggested that the bromoisobutyryl groups has been successfully introduced onto the surface of BF. Additionally, BF@PPEGMA exhibits the similar peaks of carbon (285 eV) and oxygen (533 eV) to

pristine BF, without appearance of photoelectron line for copper at 930 eV and Br 3 days at 70 eV [Fig. 2(e)]. It is indicated that CuBr was removed after the ATRP procedure and the Br signal may be overlapped by the grafted PPEGMA.²³ The C1s core level spectrum of the pristine BF and modified BF could be curve fitted with four peak components with BE at 284.9, 286.4, 287.7, and 289 eV, attributable to the C1 (C–H), C2 (C–O), C3 (O–C–O), and C4 (O–C=O), respectively. It is further noticed that the relative intensity of peak components are dependent on the surface composition of BF. The BF shows relatively stronger C3 (O–C–O) and C4 (O–C=O) peak components when compared with BIBB-immobilized BF and BF@PPEGMA. After incorporation of bromoisobutyryl groups, the C1 (C–H) peak component is more obviously observed. Furthermore, the intensity of C3 (O–C–O) and C4 (O–C=O) peak components decreases after the grafting of PPEGMA segments. It is indicated that the bromoisobutyryl groups and PPEGMA have been successfully incorporated onto the surface of BF, and the result is consistent with the FTIR analysis.

TGA analysis was further performed to analyze the thermal stability of pristine BF and modified BF as shown in Figure 3. It is noted that the pristine BF started to decompose at about 260°C , which is higher than BIBB-immobilized BF and BF@PPEGMA due to the incorporation of less thermally stable PPEGMA. The similar results were reported when itaconic acid (IA) was grafted onto cotton fabrics,²⁴ showing that the incorporation of the second component tended to make fibers thermally less stable. In particular, the major stage ($260\text{--}420^{\circ}\text{C}$) was associated to the thermal depolymerization of hemicellulose, pectin, and α -cellulose present in the fiber.²⁵

The morphology of BF and BF@PPEGMA was analyzed by SEM as shown in Figure 4. It is observed that both of the pristine and modified BF exhibited

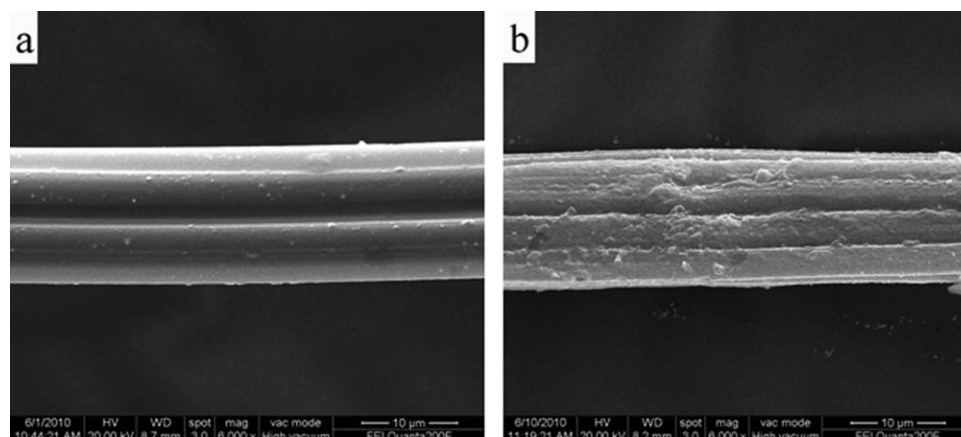


Figure 4 SEM graphs of (a) pristine BF and (b) BF@PPEGMA.

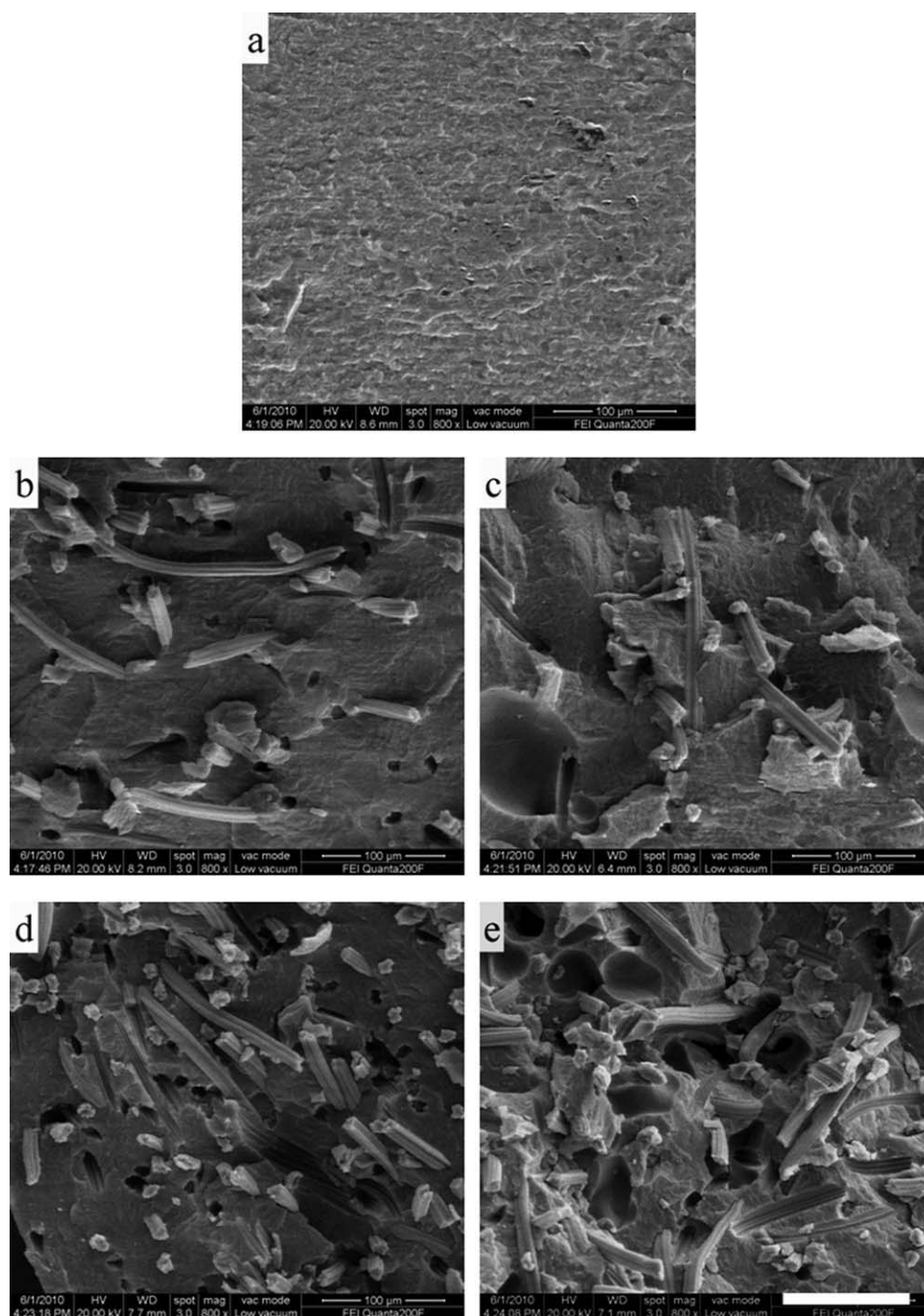


Figure 5 SEM graphs of the fractured surfaces of (a) PBS, (b) PBS/BF (95/5), (c) PBS/BF@PPEGMA (95/5), (d) PBS/BF (85/15), and (e) PBS/BF@PPEGMA (85/15).

filamentary structures. In comparison to modified BF, the pristine BF shows a relatively smooth surface. It is suggested that PPEGMA has been incorporated to BF surface, which is consistent with the results obtained from FTIR, XPS, and TGA analysis.

Morphology and tensile properties of PBS composites

The fracture surface of PBS and its composites were analyzed by SEM as shown in Figure 5. It is observed

that the pristine PBS exhibits smooth fracture surface, indicating of brittle fracture after treatment by liquid nitrogen. For PBS/BF (95/5 and 85/15) composites, the fracture surfaces are also observed to be smooth. Some of the bamboo fibers distributed in PBS matrix, whereas the others were pulled out from the matrix, leaving some holes in matrix without deformation. The BF exhibited clean and smooth surfaces without PBS residue. It is suggested that the interface interaction between pristine BF and PBS matrix is poor, due to the incompatibility between hydrophilic fibers and

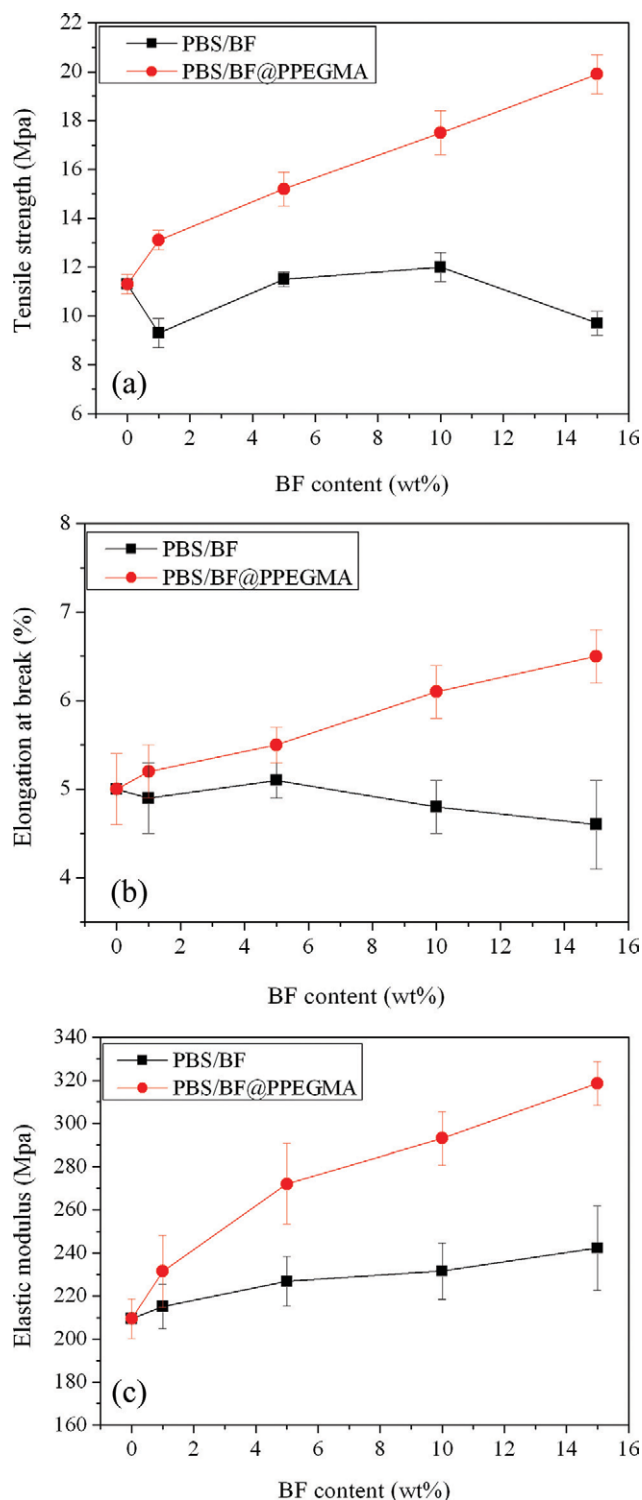


Figure 6 (a) Tensile strength, (b) elongation at break, and (c) elastic modulus versus the BF and BF@PPEGMA content of PBS/BF and PBS/BF@PPEGMA composites. [Color figure can be viewed in the online issue, which is available at wileyonlinelibrary.com.]

hydrophobic PBS matrix. In comparison, PBS/BF@PPEGMA exhibited different morphology, showing of rough surfaces. Some fibers were pulled out,

leaving holes with obvious deformation due to strong interaction between fibers and PBS matrix. It is further noticed that there are significant traces of surface scratch marks of the fibers, covered by some residual polymer. As reported by Qiu et al.,²¹ PBS and PEO were found to be completely compatible at different compositions. The PPEGMA contains PEG segments, which is supposed to be compatible with PBS. Therefore, the incorporation of PPEGMA onto BF improved interaction between BF and PBS matrix, which will eventually affect the mechanical properties of PBS composites.

Figure 6 shows the tensile strength, elongation at break, and elastic modulus of PBS and its composites versus BF or BF@PPEGMA content, and the corresponding data is listed in Table I. It is observed that incorporation of BF shows almost no beneficial effect on the values of tensile strength and elongation at break of PBS. In contrast, PBS/BF@PPEGMA composites exhibit higher values of tensile strength and elongation at break than PBS and PBS/BF composites with increase of BF@PPEGMA content. The values of elastic modulus are greatly improved by the incorporation of bamboo fibers. The elastic modulus of composites increase to about 242.3 and 318.6 MPa at BF and BF@PPEGMA content of 15%, respectively. It is indicated that the mechanical properties of PBS were significantly improved after addition of BF@PPEGMA. The grafted PPEGMA plays a vital role in determining the interfacial interaction between PBS and BF, leading to the improvement of PBS mechanical properties. Based on the SEM graphs, BF and PBS matrix showed poor interfacial adhesion, whereas the BF@PPEGMA exhibited stronger interactions with PBS matrix. Therefore, the tensile properties of composites are mainly determined by the interfacial interactions. Furthermore, the presence of hydroxyl groups on BF which has high moisture absorption made it difficult to compound with hydrophobic polymer matrix.²⁶ The reduced amount of hydroxyl groups after modification by PPEGMA is another factor affecting the tensile properties of composites. In conclusion, the modification of BF by PPEGMA is a good method to improve the interface adhesion as well as the tensile properties of composites.

Water absorption and thermal stability of PBS composites

Figure 7 exhibits the variation of water uptake of PBS/BF and PBS/BF@PPEGMA composites (25°C) as a function of time. It can be observed that, as fiber content increases, water uptake also increases. The water uptake is dependent on the hydrophilicity of BF which contains an abundance of hydroxyl groups. An interesting feature in this graph is the

TABLE I
Tensile Properties of PBS and Its Composites

Sample	Fiber content (wt %)	Tensile strength (MPa)	Elongation at break (%)	Elastic modulus (MPa)
PBS	0	11.3 ± 0.4	5.0 ± 0.4	209.5 ± 9.2
PBS/BF	1	9.3 ± 0.6	4.9 ± 0.4	215.1 ± 10.3
PBS/BF	5	11.5 ± 0.3	5.1 ± 0.2	226.8 ± 11.5
PBS/BF	10	12.0 ± 0.6	4.8 ± 0.3	231.6 ± 13.1
PBS/BF	15	9.7 ± 0.5	4.6 ± 0.5	242.3 ± 19.6
PBS/BF@PPEGMA	1	13.1 ± 0.4	5.2 ± 0.3	231.5 ± 16.7
PBS/BF@PPEGMA	5	15.2 ± 0.7	5.5 ± 0.2	272.1 ± 18.6
PBS/BF@PPEGMA	10	17.5 ± 0.9	6.1 ± 0.3	293.1 ± 12.4
PBS/BF@PPEGMA	15	19.9 ± 0.8	6.5 ± 0.3	318.6 ± 10.2

two-stage diffusion of samples, all the samples showed a similar pattern of absorption, where the samples absorbed water very rapidly during the first stage, reaching a certain value, the saturation point, where no more water was absorbed and the content of water in composites remained the same. Composites containing fibers grafted with PPEGMA showed lower water uptake than the composites containing untreated fibers. It is known that BF contains a large amount of hydroxyl groups on the surfaces, leading to absorption of high content of water. However, after modification by PPEGMA, the water absorption of PBS/BF@PPEGMA composites was lower than that of PBS/BF composites due to the change of interface properties. It is believed that a large amount of hydroxyl groups on BF were reacted and substituted by PPEGMA, which made the hydroxyl groups content decrease. Furthermore, the PPEGMA shows good compatibility with PBS

matrix, and PPEGMA molecular chains might be incorporated into the crystalline regions of PBS, making BF surfaces less hydrophilic. The decrease of hydroxyl groups, as well as strong interaction between BF and PBS matrix finally leads to the decrease of water absorption of PBS/BF@PPEGMA composites. No great reduction of water uptake ability of composites with graft BF comparing to composites with pristine BF is attributable to hydrophilicity of PPEGMA on BF surfaces.

The thermal stability of PBS composites was analyzed and the results are shown in Figure 8. It is observed that pristine BF started to decompose at relatively low temperature, and both of pristine BF and PBS exhibit a one-step degradation behavior. However, the PBS/BF and PBS/BF@PPEGMA composites show multiple stage degradation behaviors, attributing to the decomposition of bamboo fibers and PBS matrix. It is further noticed that PBS/BF@PPEGMA composites showed more weight loss stages than PBS/BF composites at the same BF content due to the existence of thermally less stable

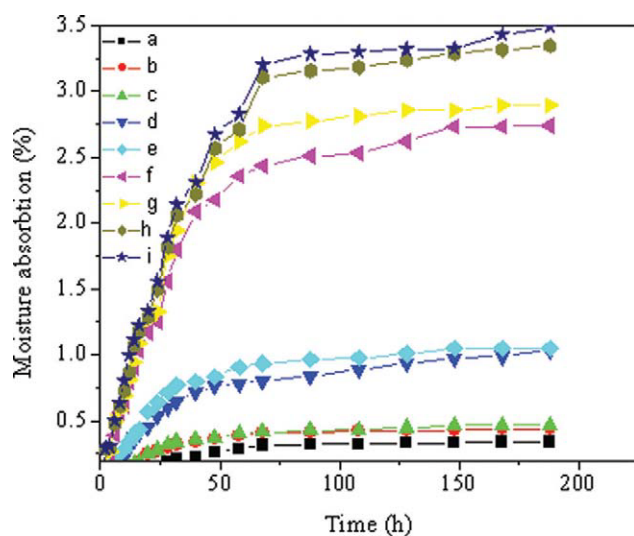


Figure 7 Effect of BF and BF@PPEGMA content on the water absorption of (a) PBS, (b) PBS/BF@PPEGMA (99/1), (c) PBS/BF (99/1), (d) PBS/BF@PPEGMA (95/5), (e) PBS/BF (95/5), (f) PBS/BF@PPEGMA (90/10), (g) PBS/BF (90/10), (h) PBS/BF@PPEGMA (85/15), and (i) PBS/BF (85/15). [Color figure can be viewed in the online issue, which is available at wileyonlinelibrary.com.]

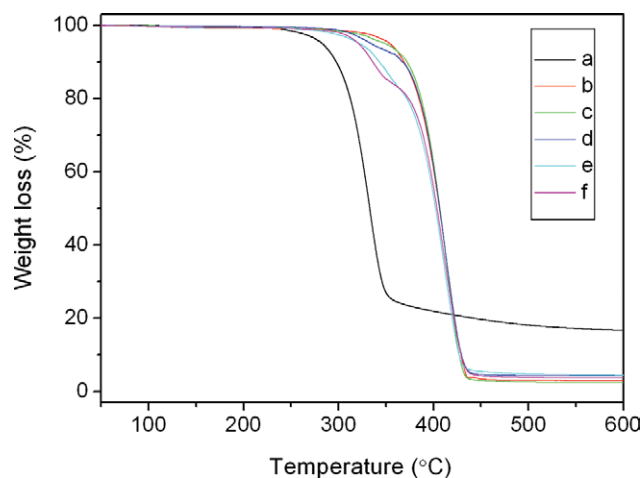


Figure 8 TGA curves of (a) BF, (b) PBS, (c) PBS/BF (95/5), (d) PBS/BF@PPEGMA (95/5), (e) PBS/BF (85/15), and (f) PBS/BF@PPEGMA (85/15). [Color figure can be viewed in the online issue, which is available at wileyonlinelibrary.com.]

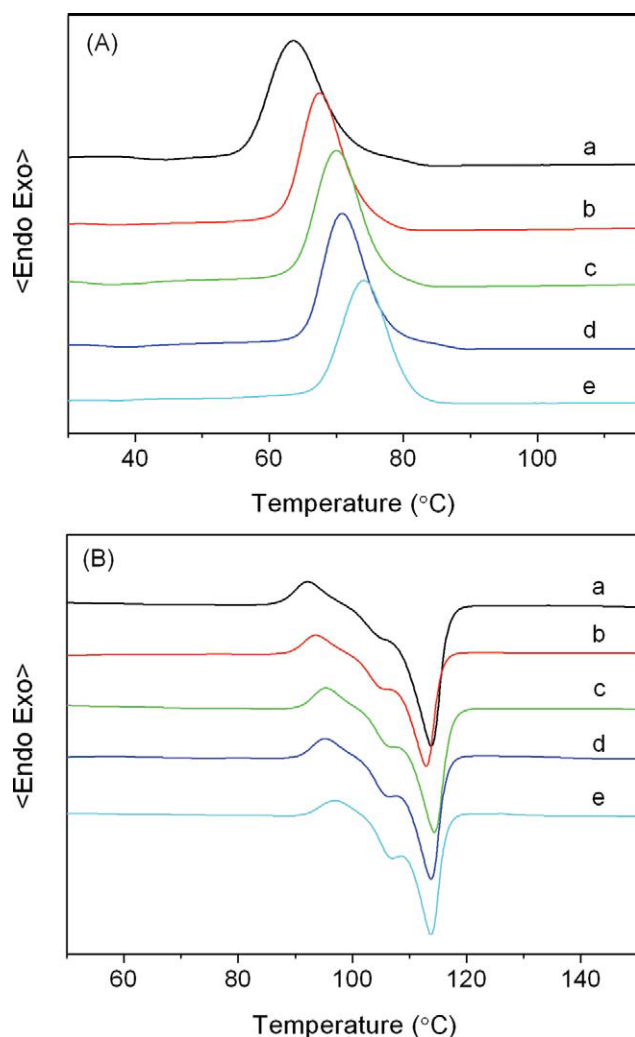


Figure 9 DSC (A) cooling and (B) heating curves for (a) PBS, (b) PBS/BF (95/5), (c) PBS/BF@PPEGMA (95/5), (d) PBS/BF (85/15), and (e) PBS/BF@PPEGMA (85/15). [Color figure can be viewed in the online issue, which is available at wileyonlinelibrary.com.]

PPEGMA segments. It is concluded that PBS composites are less thermally stable than pristine PBS.

Crystallization and melting behavior of PBS composites

It is known that the crystallization behaviors, as well as morphology of crystallites play an important role in affecting the mechanical and other properties of polymers. Figure 9 shows the crystallization and melting curves of pristine PBS and its composites, and the corresponding data is illustrated in Table II. It is observed that PBS and its composites exhibit one single crystallization peak during cooling process. Furthermore, incorporation of more content of BF facilitated crystallization at higher temperatures. The BF@PPEGMA induced PBS to crystallize at even higher temperatures. It is indicated that the existence

of BF served as nucleating agent, facilitating crystallization of PBS at high temperatures. The existence of PPEGMA improved interaction between BF and PBS, making PBS segments more flexible and easy to crystallize at higher temperatures. The PBS and its composites exhibit the similar melting behaviors, with a major melting peak at about 113.9°C and a minor melting peak at about 105.4°C. The existence of BF and BF@PPEGMA shows no significant effect on the melting behaviors of PBS matrix. However, the melting and crystallization enthalpy of PBS was influenced by incorporation of BF and BF@PPEGMA. The values of melting and crystallization enthalpy of composites are lower than those of pristine PBS.

For fiber-reinforced semicrystalline polymer composites, fiber-induced crystallization is frequently noted. In its extreme case when the nucleation density on the fiber surface is so high that crystal growth along the fiber axis is inhibited by the neighboring crystals, the crystalline structure manifests as tightly aligned spherulites growing outward from the fiber (termed transcrystallization).² The transcrystallization was observed in PHBV/flax fiber,²⁷ PHB/wood fiber,²⁸ PP/bamboo fiber,²⁹ and PP/wood flour.³⁰ However, it was not found in bamboo fiber-reinforced PBS composites.⁹ The morphology of PBS spherulites was also investigated as shown in Figure 10. It is observed that pristine PBS formed the regular spherulites, with clear interfaces between spherulites. However, the diameters of spherulites decrease after incorporation of BF and BF@PPEGMA, showing of strong nucleating effect, which is consistent with results obtained by DSC analysis. The BF could be obviously observed from POM images, and the pristine BF showed of smooth surfaces without significant interaction with PBS spherulites. In comparison, the BF@PPEGMA showed of less obvious surfaces and stronger interaction with PBS spherulites. However, no significant transcrystallization was observed, which is similar to the results reported by Kori.⁹ In conclusion, the morphology of PBS spherulites was greatly influenced by incorporation of BF and BF@PPEGMA, which eventually lead to different crystallization behaviors as observed in DSC analysis.

TABLE II
DSC Data for PBS and Its Composites

Sample	Fiber content (wt %)	T_m (°C)	T_c (°C)	ΔH_m (J/g)	ΔH_c (J/g)
PBS	0	113.9	63.6	96.1	74.2
PBS/BF	5	113.0	67.6	91.3	71.8
PBS/BF	15	113.8	70.8	89.0	73.8
PBS/BF@PPEGMA	5	114.4	70.0	82.7	67.6
PBS/BF@PPEGMA	15	113.8	74.1	71.6	66.5

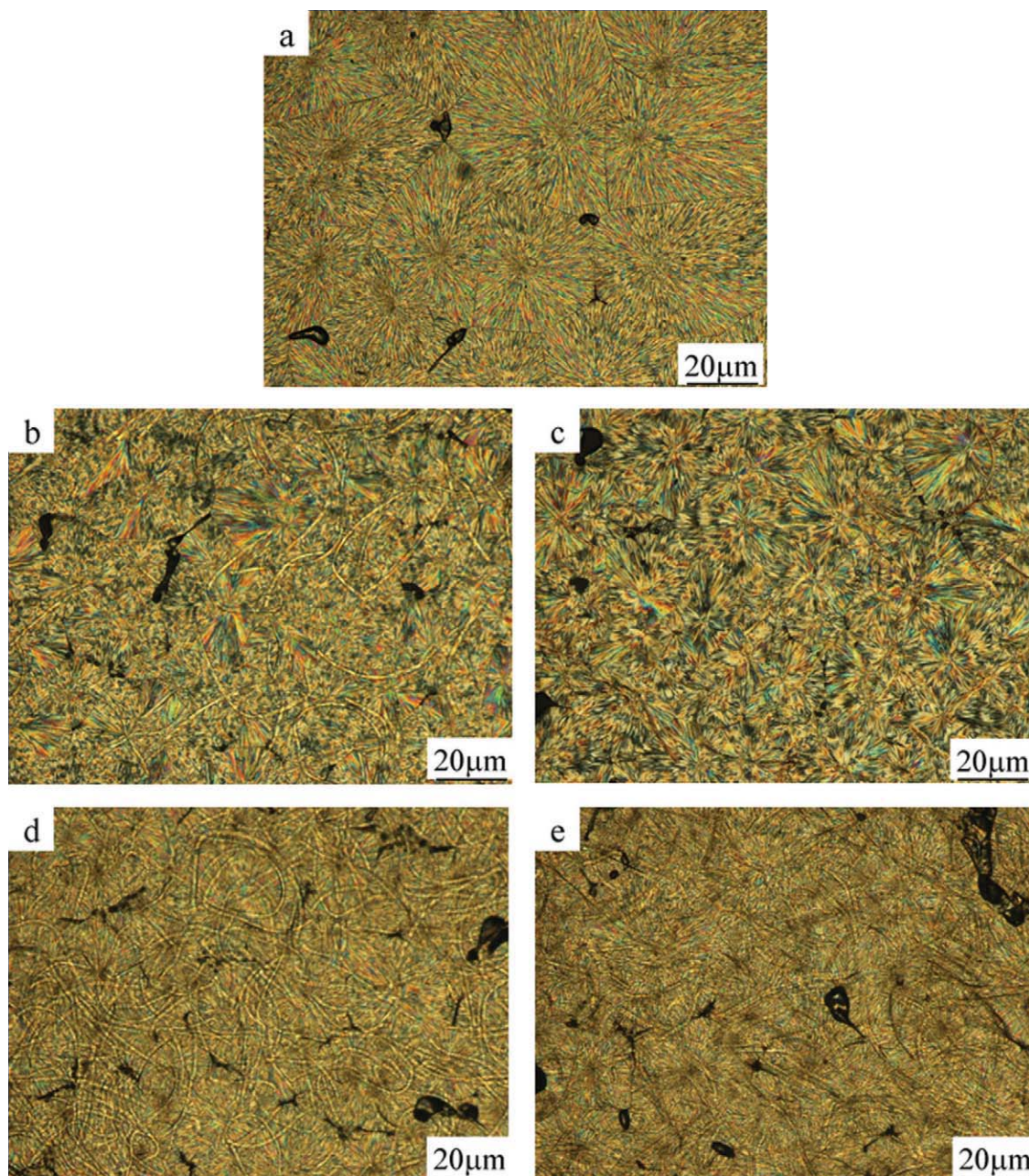


Figure 10 POM graphs of (a) PBS, (b) PBS/BF (95/5), (c) PBS/BF@PPEGMA (95/5), (d) PBS/BF (85/15), and (e) PBS/BF@PPEGMA (85/15) isothermally crystallized at 80°C for 1 h. [Color figure can be viewed in the online issue, which is available at wileyonlinelibrary.com.]

CONCLUSIONS

The PPEGMA was successfully grafted onto BF via esterification and atom transfer radical polymerization. The BF@PPEGMA was found to have a stronger adhesion with PBS matrix than pristine BF as observed from SEM analysis, due to interaction between PPEGMA and PBS. The tensile strength, elongation at break, as well as elastic modulus of PBS/BF@PPEGMA composites was higher than those of PBS/BF composites due to stronger interfa-

cial interactions between modified BF and PBS matrix. The water absorption of PBS/BF@PPEGMA composites was lower than that of PBS/BF composites due to change of interface properties. The BF and BF@PPEGMA facilitated crystallization of PBS at higher temperatures, serving as the nucleation agent. No significant transcrystallization was observed for PBS composites, and the BF@PPEGMA showed of better interaction with PBS as observed from POM.

References

1. Auras, R.; Harte, B.; Selke, S. *Macromol Biosci* 2004, 4, 835.
2. Jiang, L.; Huang, J.; Qian, J.; Chen, F.; Zhang, J.; Wolcott, M. P.; Zhu, Y. *J Polym Environ* 2008, 16, 83.
3. Shin, F. G.; Xian, X. J.; Zheng, W. P.; Yipp, M. W. *J Mater Sci* 1989, 24, 3483.
4. Katona, J. M.; Sovilj, V. J.; Petrovic, L. B. *Carbohydr Polym* 2010, 79, 563.
5. Chen, H.; Miao, M.; Ding, X. *Compos Part A Appl Sci Manuf* 2009, 40, 2013.
6. Das, M.; Pal, A.; Chakraborty, D. *J Appl Polym Sci* 2006, 100, 238.
7. Chen, X.; Guo, Q.; Mi, Y. *J Appl Polym Sci* 1998, 69, 1891.
8. Wang, H.; Chang, R.; Sheng, K.; Adl, M.; Qian, X. *J Bionic Eng* 2008, 5, 28.
9. Kori, Y.; Kitagawa, K.; Hamada, H. *J Appl Polym Sci* 2005, 98, 603.
10. Lee, S. H.; Wang, S. *Compos Part A Appl Sci Manuf* 2006, 37, 80.
11. Huda, M. S.; Drzal, L. T.; Mohanty, A. K.; Misra, M. *Compos Part B Eng* 2007, 38, 367.
12. Gassan, J.; Bledzki, A. K. *J Appl Polym Sci* 1999, 71, 623.
13. Acha, B. A.; Reboredo, M. M.; Marcovich, N. E. *Polym Int* 2006, 55, 1104.
14. Liu, L.; Yu, J.; Cheng, L.; Qu, W. *Compos Part A Appl Sci Manuf* 2009, 40, 669.
15. Zhang, Y. C.; Wu, H. Y.; Qiu, Y. P. *Bioresour Technol* 2010, 101, 7944.
16. Gupta, K. C.; Khandekar, K. *J Appl Polym Sci* 2006, 101, 2546.
17. Hafrén, J.; Córdova, A. *Macromol Rapid Commun* 2005, 26, 82.
18. Daly, W. H.; Evenson, T. S.; Iacono, S. T.; Jones, R. W. *Macromol Symp* 2001, 174, 155.
19. Roy, D.; Guthrie, J. T.; Perrier, S. *Macromolecules* 2005, 38, 10363.
20. Carlmark, A.; Malmstrom, E. *J Am Chem Soc* 2002, 124, 900.
21. Qiu, Z. B.; Yan, C. Z.; Lu, J. M.; Yang, W. T.; Ikehara, T. I.; Nishi, T. *J Phys Chem B* 2007, 111, 2783.
22. Krouit, M.; Bras, J.; Belgacem, M. N. *Eur Polym Mater* 2008, 44, 4074.
23. Peng, X. M.; Chen, Y. W.; Li, F.; Zhou, W. H.; Hu, Y. H. *Appl Surf Sci* 2009, 255, 7158.
24. Sabaa, M. W.; Mokhtar, S. M. *Polym Test* 2002, 21, 337.
25. De Rosa, I. M.; Kenny, J. M.; Puglia, D.; Santulli, C.; Sarasini, F. *Compos Sci Technol* 2010, 70, 116.
26. Islam, M. N.; Haque, M. M.; Huque, M. M. *Ind Eng Chem Res* 2009, 48, 401.
27. Wong, S. S.; Shanks, R.; Hodzic, A. *Macromol Mater Eng* 2009, 287, 647.
28. Reinsch, V. E.; Kelley, S. S. *J Appl Polym Sci* 1997, 64, 1785.
29. Mi, Y. L.; Chen, X. Y.; Guo, Q. P. *J Appl Polym Sci* 1997, 64, 1267.
30. Harper, D.; Wolcott, M. *Compos A* 2004, 35, 385.